JOURNAL OF VIROLOGY, Apr. 2011, p. 3375–3384 Vol. 85, No. 7
0022-538X/11/$12.00 doi:10.1128/JVI.01952-10

Human Cytomegalovirus UL97 Kinase and Nonkinase Functions Mediate Viral Cytoplasmic Secondary Envelopment▽

Miri D. Goldberg,[1,2] Alik Honigman,[2] Jacob Weinstein,[1,2] Sunwen Chou,[3] Albert Taraboulos,[2] Alexander Rouvinski,[2] Vera Shinder,[4] and Dana G. Wolf[1]*

Hadassah Hebrew University Medical Center[1] and IMRIC,[2] The Hebrew University-Hadassah Medical School, Jerusalem, Israel; VA Medical Center and Oregon Health and Science University, Portland, Oregon[3]; and Weizmann Institute of Life Sciences, Rehovot, Israel[4]

Received 15 September 2010/Accepted 10 January 2011

Previous studies have revealed critical roles for the human cytomegalovirus (HCMV) UL97 kinase in viral nuclear maturation events. We have shown recently that UL97 affects the morphology of the viral cytoplasmic assembly compartment (AC) (M. Azzeh, A. Honigman, A. Taraboulos, A. Rouvinski, and D. G. Wolf, Virology 354:69–79, 2006). Here, we employed a comprehensive ultrastructural analysis to dissect the impact of UL97 on cytoplasmic steps of HCMV assembly. Using UL97 deletion (ΔUL97) and kinase-null (K355M) mutants, as well as the UL97 kinase inhibitor NGIC-I, we demonstrated that the loss of UL97 kinase activity resulted in a unique combination of cytoplasmic features: (i) the formation of pp65-rich aberrant cytoplasmic tegument aggregates, (ii) distorted intracytoplasmic membranes, which replaced the normal architecture of the AC, and (iv) a paucity of cytoplasmic tegumented capsids and dense bodies (DBs). We further showed that these abnormal assembly intermediates did not result from impaired nuclear capsid maturation and egress *per se* by using 2-bromo-5,6-dichloro-1-(β-*d*-ribofuranosyl) benzimidizole (BDCRB) to induce the artificial inhibition of nuclear maturation and the nucleocytoplasmic translocation of capsids. The specific abrogation of UL97 kinase activity under low-multiplicity-of-infection conditions resulted in the improved release of extracellular virus compared to that of ΔUL97, despite similar rates of viral DNA accumulation and similar effects on nuclear capsid maturation and egress. The only ultrastructural correlate of the growth difference was a higher number of cytoplasmic DBs, tegumented capsids, and clustered viral particles observed upon the specific abrogation of UL97 kinase activity compared to that of ΔUL97. These combined findings reveal a novel role for UL97 in HCMV cytoplasmic secondary envelopment steps, with a further distinction of kinase-mediated function in the formation of the virus-induced AC and a nonkinase function enhancing the efficacy of viral tegumentation and release.

Human cytomegalovirus (HCMV), a ubiquitous betaherpesvirus, is a major cause of disease in immunocompromised individuals and a leading cause of congenital infection (57). The HCMV virion consists of a DNA-containing capsid, which is embedded in a tegument layer, and a lipid envelope, which contains the virus-encoded glycoproteins (57). The HCMV infection of cells in culture generates infectious virions, as well as dense bodies (DBs; nonreplicating particles composed of tegument surrounded by an envelope) and noninfectious enveloped particles lacking viral DNA (57, 80).

During capsid maturation in the nucleus, large concatemeric DNA intermediates are cleaved to genome-length units and packaged into preformed capsids via the DNA cleavage/packaging machinery (57). The current model suggests that assembled nucleocapsids bud through the inner nuclear membrane, acquiring a primary envelope layer. Subsequent shuttling into the cytoplasm and cytoplasmic assembly steps involve deenvelopment and the budding of nucleocapsids into virus-induced concentric layers of cytoplasmic vesicles derived from endosomes, the *trans*-Golgi network, and the Golgi apparatus and endoplasmic reticulum (ER) Golgi intermediate compartment, together regarded as the viral assembly compartment (AC), where final tegumentation and secondary envelopment occurs (13, 22, 25, 29, 51, 57, 59, 69, 77).

Mature virions and DBs are carried by the cellular vesicle transport machinery to the plasma membrane for exocytic release (57). The mechanisms mediating these final steps of cytoplasmic assembly, including tegument formation and envelopment, particle transport, and release, are still largely unknown.

The HCMV UL97 gene product is a serine/threonine kinase, originally discovered because of its unique ability to phosphorylate the nucleoside analog ganciclovir, thus mediating its antiviral activity (46, 73). The UL97 kinase has recognizable homologs in all herpesviruses, including the herpes simplex virus (HSV) UL13, the varicella zoster virus (VZV) ORF47, the Epstein-Barr virus (EBV) BGLF4, the human herpesvirus 6 (HHV-6) U69, the human herpesvirus 8 (HHV-8) ORF36, murine cytomegalovirus (CMV) M97, and rat CMV R97 (52). These proteins modify common cellular and conserved viral targets, such as the cellular elongation factor 1 delta (36), the nuclear lamins (16, 45), and the viral DNA polymerase processivity factor (17, 84), but they are functionally divergent (68). The alphaherpesvirus homologs have been shown to phosphorylate immediate-early and late viral proteins and, although proven nonessential for viral growth in cell culture, have been implicated in the regulation of all phases of viral infection as well as in affecting tissue tropism (35, 37, 58, 60, 66). Other serine/threonine kinases, the US3 kinases (ORF66 in VZV), are found among members of the alphaherpesvirus subfamily (67). The US3 kinases have been shown to promote

* Corresponding author. Mailing address: Clinical Virology Unit, Dept. of Clinical Microbiology & Infectious Diseases, Hadassah Hebrew University Medical Center, Jerusalem, Israel 91120. Phone: 972-2-6777890. Fax: 972-2-6427921. E-mail: dana.wolf@ekmd.huji.ac.il.

▽ Published ahead of print on 19 January 2011.

the egress of nucleocapsids from the nucleus, sustain viral long-distance axon transport, and influence various host cell processes, including actin dynamics, apoptosis, nuclear membrane architecture, and intracellular signaling (21, 23, 67).

The UL97 gene product is expressed early during infection and is a constituent of the viral tegument (53, 62, 79). This protein plays a crucial role in viral replication, and a UL97 deletion results in severe replication deficits (62, 64).

The UL97 kinase has been shown to be the target of the new experimental antiviral drug maribavir (7, 8). It has been shown to phosphorylate several viral proteins, including itself, the viral DNA polymerase processivity factor ppUL44, the major tegument protein pp65, and the viral nuclear mRNA export factor pUL69 (3, 34, 41, 48, 76). Identified cellular targets of UL97 kinase include the large subunit of RNA polymerase II, eukaryotic elongation factor 1Δ, P32, lamins A/C, and the retinoblastoma tumor suppressor protein (Rb) (4, 27, 30, 36, 49, 65).

Previous studies of replication-deficient null mutants of UL97 have shown a complex role of UL97 kinase in nuclear steps of the viral life cycle, namely, in DNA synthesis, DNA encapsidation, capsid maturation, and nuclear egress (27, 40, 49, 55, 82). More recently, we have shown that UL97 affects the morphology of the viral cytoplasmic assembly compartment (2). This finding, pointing to a cytoplasmic role for UL97, prompted us to dissect the cytoplasmic events of HCMV assembly that are governed by UL97 using comprehensive ultrastructural analysis. In view of the multiple roles played by this protein, we further sought to determine whether the individual multistep defects exerted by the absence of UL97 all are due to the loss of its kinase activity. Using UL97 mutants and specific viral inhibitors, we demonstrate that UL97 is involved in HCMV secondary envelopment and tegumentation in the cytoplasm via both kinase- and nonkinase-mediated functions.

MATERIALS AND METHODS

Cells, viruses, antibodies, and drugs. HCMV strain AD169 (wild-type HCMV) was obtained from the American Type Culture Collection. Two independently engineered isolates of RCΔ97 (UL97 deletion mutant; ΔUL97), RCΔ97.08 and RCΔ97.19, derived from AD169 and containing the *Escherichia coli lacZ* and *gpt* genes replacing most of UL97 as described previously (64), were generously provided by Mark Prichard (University of Alabama, Birmingham). T2819, a point mutant in which the UL97 kinase activity was specifically abrogated by a K355M substitution of the kinase catalytic lysine (50), was constructed as described below. All virus strains were propagated in human foreskin fibroblasts (HFF) as described previously (82). Primary mouse monoclonal antibodies (MAbs) against HCMV immediate-early protein IE1/2, pp28, pp65, and glycoprotein B (gB) were purchased from Chemicon (Rosemont, IL) and Virusys Corporation (Taneytown, MD). The secondary antibody was anti-mouse IgG coupled to a 10-nm gold particle (Electron Microscopy Sciences, Hatfield, PA). The antiviral drug 2-bromo-5,6-dichloro-1-(β-*d*-ribofuranosyl) benzimidizole (BDCRB) (20 μM; a kind gift from John Drach, University of Michigan) or NGIC-I (0.5 μM; Calbiochem, Germany) was added 1 h after virus adsorption to cells, which subsequently were incubated in the presence of the drug for 96 h postinfection (hpi) unless specified differently. For block-release experiments, drug-treated cultures were washed five times with phosphate-buffered saline (PBS) and then further incubated for the indicated times after drug release in drug-free medium. Viral growth curves were carried out in freshly plated HFF infected at a specified multiplicity of infection (MOI). Samples of infected cell supernatants were removed at designated time points and stored at −80°C before titration by plaque assay on HFF.

Construction of UL97 K355M mutant (strain T2819). The *Escherichia coli* strain SW102, containing a deleted *galK* gene and temperature-inducible genetic elements *exo*, *bet*, and *gam*, which enable the transient high-frequency homologous recombination of hosted bacterial artificial chromosomes (BACs) (81), and a *galK* expression plasmid vector (81), was obtained from the Biological Resources Branch of the National Cancer Institute (http://recombineering.ncifcrf.gov). The HCMV strain AD169-derived BAC HB5 was obtained from Messerle et al. (10). HB5 was electroporated into *E. coli* strain SW102, and 42°C heat-induced, electrocompetent bacteria containing the BAC were prepared as described previously (81) and transformed with the plasmid-derived *galK* expression cassette flanked by UL97 coding sequences, such that homologous recombination with HB5 resulted in the removal of the UL97 region DNA sequence between the BamHI restriction site at 140547 (UL97 codon 23) and the XhoI site at 142713 (past the end of the UL97 coding sequence). The recombinant BAC HB5-B2 was isolated by selective growth on minimal medium containing *d*-galactose (81) and purified by retransformation into *E. coli* SW102. DNA from an isolated colony was checked by PCR for the presence of the intended *galK* gene and the absence of the removed UL97 sequence. The *galK*-containing BAC HB5-B2 then was recombineered (81) again with a subclone of strain AD169 containing the UL97 region (plasmid SC102; nucleotides 139690 to 144436) modified to contain the K355M mutation (20). After electroporation into heat-induced *E. coli* SW102 containing HB5-B2, recombinant BACs that had lost *galK* and gained the K355M mutation were isolated by counterselection with 2-deoxygalactose (81). Recombinant BACs were restreaked for isolation in host bacteria and qualified by having intact restriction digest patterns (e.g., with XbaI or HindIII) identical to that of HB5 and by PCR and sequencing to show the presence of the mutation K355M and the absence of *galK* sequences. A qualifying BAC, HB5-B8, was grown in *E. coli* SW102, and the extracted DNA (~3 μg) was transfected (using Fugene 6 reagent; Roche) into a human foreskin fibroblast culture monolayer in a six-well cluster plate. After the serial passage of the cells to T25 and T75 flasks, HCMV cytopathic effect was observed starting 2 weeks later (strain T2819), and it had the characteristic appearance of multiple small intranuclear inclusions typical of UL97-deficient strains (63). Viral DNA extracted from the infected fibroblasts was sequenced throughout the coding sequences of UL97 and UL27 to confirm the presence of the mutation UL97 K355M and the absence of any other unintended changes elsewhere in UL97 or UL27 (19).

Transmission electron microscopy (EM). (i) Standard fixation. HFF cells grown on coverslips in six-well plates were infected at an MOI of 0.1. At 96 hpi, cells were fixed in 2.5% glutaraldehyde and 2% paraformaldehyde in 0.1 M cacodylate buffer (pH 7.4) at room temperature for 1 h, washed, and postfixed with 1% osmium tetroxide in the same buffer for 1 h at room temperature. After en bloc staining with 2% aqueous uranyl acetate for 1 h at room temperature, the samples were dehydrated through a graded ethanol series and embedded in Epon 812.

(ii) HPF fixation. Cells grown on sapphire disks in six-well plates were infected at an MOI of 0.1. At 96 hpi, cells were fixed by high-pressure freezing (HPF) in a Bal-Tec HPM10 apparatus. Frozen samples were transferred to a Leica AFS apparatus (Vienna, Austria) and freeze substituted in acetone containing 0.1% glutaraldehyde and 0.1% uranyl acetate at −90°C for 72 h. The samples then were washed in ethanol and embedded in HM20 resin at −30°C under UV light.

Ultrathin sections (70 to 90 nm) were prepared with the Ultramicrotome Leica UCT (Vienna, Austria), analyzed at 120 kV with a Tecnai 12 transmission electron microscope (FEI, Eindhoven, Netherlands), and digitized with a Megaview III charge-coupled-device camera using AnalySIS software (AnalySIS, Munster, Germany).

(iii) Immunogold labeling. Following HPF, the sections were washed with PBS with 0.2% glycine. After 20 min of blocking using 0.1% glycine, 1% gelatin, 0.1% Tween 20, and 1% bovine serum albumin (BSA) in PBS, the indicated primary antibody was added to the cells in an appropriate dilution in the blocking buffer and incubated for 1.5 to 2 h at room temperature or overnight at 4°C. The secondary gold-labeled antibody was added and incubated for 30 to 40 min at room temperature. The sections then were rinsed once with PBS and six times with double-distilled water.

Analysis of viral DNA accumulation. To measure the accumulation of viral DNA, total cellular DNA was extracted at specified times from virus-infected and mock-infected HFF using the QIAamp blood minikit extraction kit (Qiagen, Hilden, Germany). Viral DNA was quantified by quantitative real-time PCR (RT PCR), using primers and probe derived from the gB gene as previously described (9). The assay demonstrated a linear quantitation for a 6-log range (71).

Amplification and sequencing of the HCMV UL97 gene. Direct PCR sequencing was performed as described previously by using overlapping primer pairs encompassing nucleotides 1207 to 1979 (83).

RESULTS

A role for UL97 in cytoplasmic steps of secondary envelopment and tegumentation. (i) Formation of aberrant cytoplasmic tegument aggregates and distorted intracytoplasmic membranes in the absence of UL97. To evaluate the effect of UL97

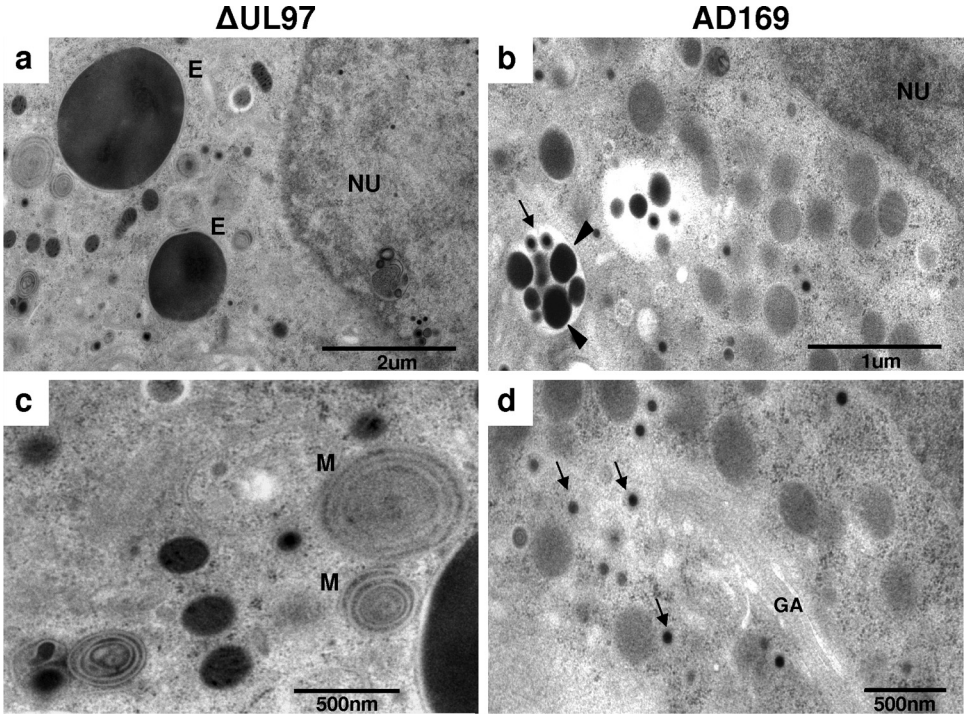

FIG. 1. Transmission electron microscopy of ΔUL97 (a and c)- and AD169 (b and d)-infected HFF at 96 hpi. The arrow in panel b points to viral particles clustered within cytoplasmic vacuoles. The arrowheads point to dense bodies. The arrows in panel d point to tegumented C capsids. E, electron-dense structures; M, ovoid membrane stacks; GA, Golgi apparatus; NU, nucleus. Cells in the presented micrographs were fixed by high-pressure freezing.

deletion on the presence and distribution of cytoplasmic assembly intermediates, we have employed transmission EM on ultrathin sections of HFF infected with ΔUL97 (RCΔ97.08) or wild-type virus (AD169) at 96 hpi. Major differences were found in the comparison of the cytoplasmic morphology of cells infected by the two viruses (Fig. 1). In ΔUL97-infected cells, only a few DNA-containing capsids and dense bodies could be seen in the cytoplasm, with the notable complete absence of viral particle clusters (Fig. 1a and c and Table 1). No release of viral particles at the cell surface could be detected. These findings were in contrast to those for cells infected with the wild-type virus, which demonstrated all cytoplasmic stages of the virus morphogenesis, including budding and envelopment of DNA-containing nucleocapsids in Golgi-derived membrane vesicles and the formation of tegumented C capsids along with clusters of mature viral particles and dense bodies within vesicles (Fig. 1b and d and Table 1), with the release of virions and DBs at the cell surface (not shown). Additional striking features found exclusively in ΔUL97-infected cells included (i) the formation of abnormally large (1 to 8 μm diameter) cytoplasmic electron-dense structures (Fig. 1a), occasionally surrounded by a thin membrane or associated with viral particle intermediates, and (ii) distorted intracytoplasmic membrane stacks, which appeared as ovoid tightly packed multilayer onion-like structures (Fig. 1a and c). Importantly, similar findings were noted with the independently engineered UL97 deletion mutant RCΔ97.19 (data not shown), further supporting the relatedness of the observed phenotype to the UL97 deletion.

To characterize the aberrant intracytoplasmic structures formed in the absence of UL97 and their relation to viral assembly intermediates, we have used immunogold labeling with antibodies directed against the viral structural proteins pp65, pp28, and gB (Fig. 2). Immunoelectron microscopy revealed the diffuse heavy staining of the electron-dense structures with antibodies for the major tegument protein pp65 (Fig. 2a), with comparable yet mainly peripheral staining for the tegument protein pp28 (Fig. 2b) and no specific staining for

TABLE 1. Quantitative measurements of viral assembly intermediates in HFF infected with wild-type and mutant HCMV strains[a]

HCMV strain	Empty:DNA-containing capsids in the nucleus (mean ratio)	Cytoplasmic tegumented capsids (mean no./μm^2 ±SE)	Cytoplasmic dense bodies (mean no./μm^2 ±SE)	Cytoplasmic VPC vacuole status	
				No. per infected cell	% of infected cells containing VPC
AD169	1:1.5	1.3 ± 0.3	0.6 ± 0.3	1–2	100
ΔUL97	3:1	0.02 ± 0.04	0.04 ± 0.01	0	0
T2819	3:1	0.2 ± 0.04	0.2 ± 0.1	1	25

[a] Quantitative measurements were based on analysis of 100 representative fields from different sections. SE, standard errors. VPC, virus particle cluster.

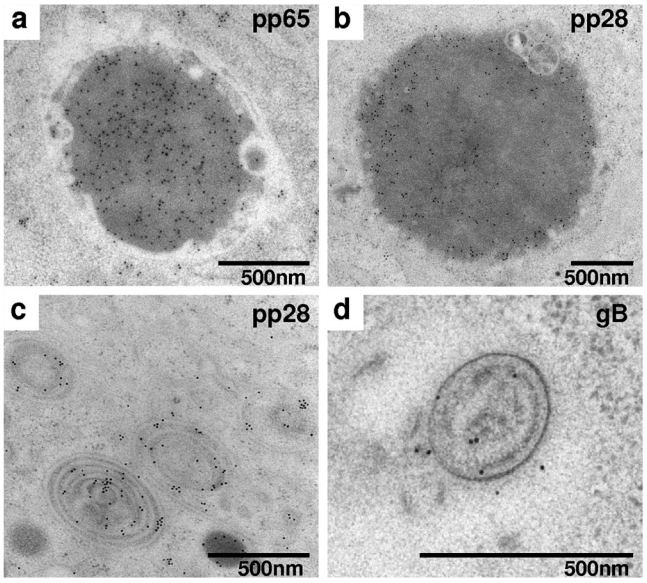

FIG. 2. Immunoelectron microscopy detection of HCMV proteins in ΔUL97-infected HFF at 96 hpi. Ultrathin sections prepared following high-pressure freezing were subjected to immunogold labeling with anti-pp65 (a), pp28 (b and c), and gB (d) antibodies. The specific staining of the cytoplasmic electron-dense structures (a and b) and ovoid membrane stacks (c and d) is shown.

gB (gB could be detected in mature extracellular viral particles in wild-type infected cells; data not shown). These findings suggest that the electron-dense structures formed in the absence of UL97 represent aberrant cytoplasmic tegument aggregates composed mainly of pp65. The impacted membranes showed abundant specific staining for the membrane-associated tegument protein pp28 (Fig. 2c), with sparse staining for gB (Fig. 2d) and no staining for pp65 (not shown). Taken together, the paucity of the predicted cytoplasmic assembly intermediates, including enveloped particle forms and exocytic vesicle clusters in the cytoplasm of ΔUL97-infected cells, along with the formation of aberrant tegument and membrane aggregates, suggest the involvement of UL97 in cytoplasmic assembly steps.

(ii) The defect in cytoplasmic assembly in ΔUL97-infected cells does not result from impaired capsid maturation and nuclear egress *per se*. To examine whether the observed cytoplasmic effects could result from the block in nuclear maturation and egress in the absence of UL97, wild-type HCMV-infected cells were cultured for 96 h in the presence of 20 μM 2-bromo-5,6-dichloro-1-(β-*d*-ribofuranosyl) benzimidizole (BDCRB), which is known to inhibit the maturation and nucleocytoplasmic translocation of capsids (75, 78), and examined by transmission EM. The BDCRB block of wild-type-infected cells resulted in the expected inhibition of capsid maturation and nuclear egress, as revealed by the nuclear accumulation of empty capsids and the absence of capsid forms or mature virions in the cytoplasm (Fig. 3a to c). However, despite the abrogation of nuclear maturation steps, none of the aberrant cytoplasmic structures observed in the absence of UL97 could be detected (compare Fig. 1a and c to Fig. 3c). Interestingly, a more prominent feature in the cytoplasm of BDCRB-treated cells was the formation of numerous DBs, which could be seen both as free particles and in clusters within cytoplasmic vacuoles, transported and released into the extracellular space (Fig. 3c and d). These results demonstrate that the abrogation of nuclear encapsidation and egress by itself is not the cause of the aberrant cytoplasmic features and the paucity of tegumented DB forms observed in the absence of UL97. Furthermore, combined treatment with BDCRB and the UL97 inhibitor NGIC-I resulted in the nuclear accumulation of empty capsids (similar to that observed in BDCRB-treated cells; data not shown) with the formation of ΔUL97-like tegument aggregates and aberrant membrane stacks (Fig. 3e and f). These findings confirm that the defect in cytoplasmic assembly in the absence of UL97 reflects its involvement in cytoplasmic assembly steps and does not represent a direct consequence of impaired nuclear maturation.

UL97 has both kinase-mediated and nonkinase functions in viral replication. (i) Specific abrogation of UL97 kinase activity results in improved release of extracellular virus compared to the effect of UL97 deletion. The multiple defects displayed by the UL97 deletion mutant, involving both nuclear and cytoplasmic maturation steps, raised the question of whether they all are due to the loss of kinase activity. To delineate the specific contribution of the UL97 kinase activity to viral replication, the growth rate of the UL97 deletion mutant was compared to that of a point mutant (K355M; strain T2819) in which the UL97 kinase activity was specifically abrogated. The K355M point mutation abrogates the kinase catalytic lysine, and in the case of UL97 it has been shown to result in the complete inactivation of the kinase activity (30, 50, 63). HFF were infected with AD169, ΔUL97, and T2819 at either high (≥1 PFU/cell) or low (≤0.1 PFU/cell) multiplicity, and virus titers were determined in the supernatant at different times postinfection. The MOI equivalence of the different viruses in comparative experiments was further confirmed by the immunofluorescence staining of HFF infected with the different strains for the immediate-early protein IE1/2 at 24 hpi. After high-multiplicity infection, ΔUL97 and T2819 accumulated to similar levels, both demonstrating ~2 log reduction in viral yield compared to the level of AD169 (data not shown). This finding was consistent with results reported previously (26, 30). At an MOI of ≤0.1, the titer of cell-associated virus measured in infected HFF lysates remained comparable between ΔUL97 and T2819 (Fig. 4a). However, the release of infectious virus from T2819 was lower by one order of magnitude than that of AD169 and higher by one order of magnitude than that of ΔUL97-infected cells (Fig. 4b). Similar results were obtained using independently derived deletion mutants RCΔ97.08 and RCΔ97.19.

Sequence analysis of DNA extracted from T2819 viral stock and infected cells confirmed the presence of pure K355M mutant population, thus excluding the presence of a reversion mutation with a mixed viral population as a potential cause for the intermediate growth phenotype of T2819. To further confirm that the growth difference between ΔUL97 and T2819 was related to the specific abrogation of UL97 kinase activity in T2819, we employed the UL97 kinase inhibitor NGIC-I as previously described (2). NGIC-I (0.5 μM) was added to the growth medium following AD169, ΔUL97, or T2819 adsorption to the cells. The infected cells were further incubated in the presence of the drug for 96 h.

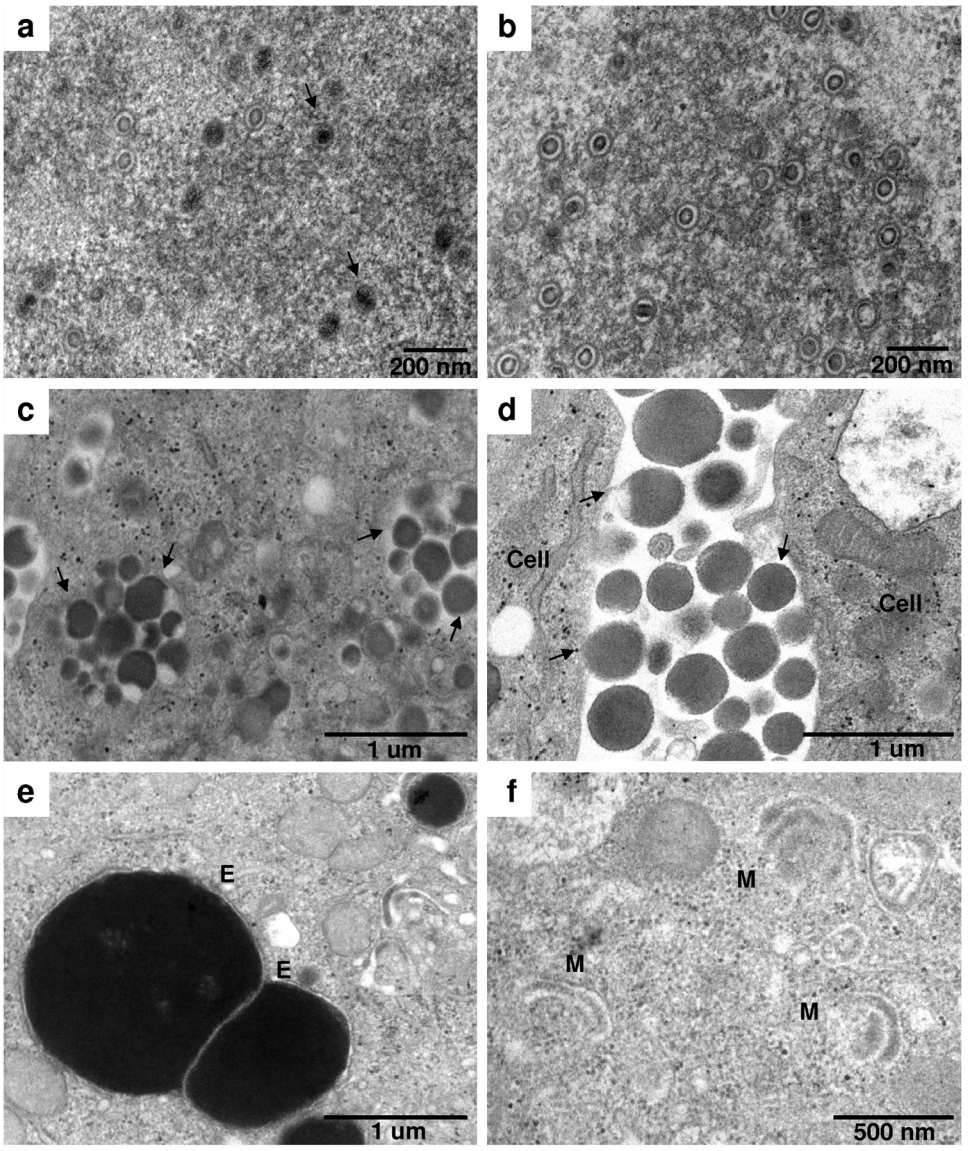

FIG. 3. Transmission electron microscopy of AD169-infected HFF treated with BDCRB and NGIC-I at 96 hpi. (a and b) Nucleus; (c, e, and f) cytoplasm; (d) intercellular space; (b to d) BDCRB-treated infected HFF; (e and f) BDCRB- and NGIC-I-treated infected HFF. Arrows in panel a point to C capsids. Arrows in panels c and d point to dense bodies. E, electron-dense structures; M, ovoid membrane stacks. Cells in the presented micrographs were fixed by standard fixation.

At low MOI, NGIC-I-treated AD169-infected cells yielded virus titers similar to those of the T2819-infected cells, with a 1-log increase compared to titers of ΔUL97-infected cells (Fig. 4b). The consistent growth advantage of the kinase-null or kinase-abrogated virus over the UL97 deleted mutant suggested that the kinase activity is not responsible for all of the replication steps mediated by the UL97 protein, and that an additional nonkinase function contributes to the efficiency of virus release under low-MOI conditions.

(ii) Viral DNA accumulation. Since UL97 has been shown to play a role in viral DNA synthesis, we examined whether the observed replication difference between the kinase-abrogated K355M mutant and ΔUL97 results from different rates of DNA synthesis. The intracellular accumulation of viral DNA was evaluated by quantitative RT PCR. Overall, DNA accumulation in cells infected with the two mutant viruses was similar and demonstrated an up to 1-log decrease in viral DNA synthesis compared to results for the wild-type virus (Fig. 4c). Thus, the inhibition of DNA synthesis appeared to be completely mediated by the abrogated kinase activity of UL97 and could not explain the observed replication difference between the deletion and kinase-null mutants.

Kinase-mediated and nonkinase functions of UL97 in the late phase of viral replication. We investigated the effect of UL97 deletion versus kinase abrogation during the late phase of viral replication by employing a reversible block with BDCRB as previously described (82). BDCRB is known to inhibit the cleavage of concatemeric viral DNA molecules as well as the packaging of progeny DNA into nucleocapsids (78, 82). As we have shown previously, BDCRB treatment results

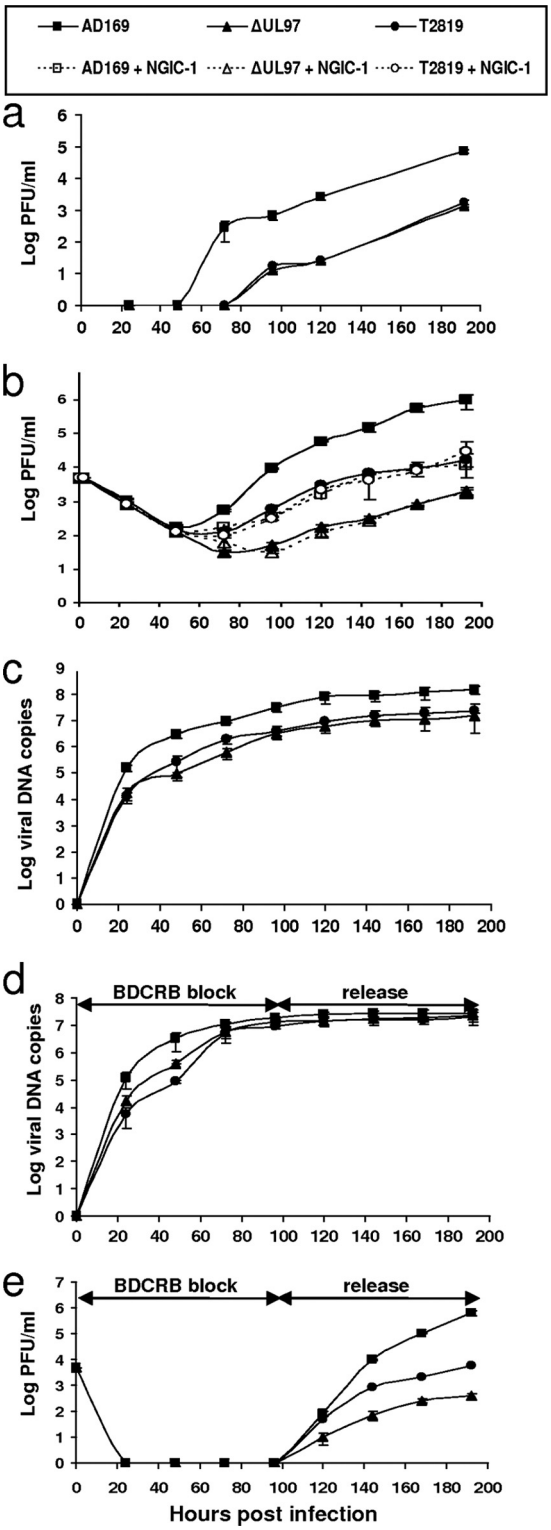

FIG. 4. Viral growth and DNA accumulation curves for ΔUL97, T2819, and AD169. HFF were infected at an MOI of 0.1 PFU/cell, and titers of the cell-associated virus in infected cells (a), the resulting progeny virus in the supernatant (b and e), or the accumulation of viral DNA in cell lysates (c and d) were determined at the indicated times. As indicated in panel b, growth curves also were obtained during treatment with NGIC-1 (broken lines). Panels d and e show the viral DNA accumulation (d) and growth curves (e) during BDCRB block release.

in the accumulation of only noncleaved DNA intermediates, thus synchronizing DNA accumulation in both the wild type and ΔUL97 mutant (82). Indeed, during BDCRB block (for 96 hpi), viral DNA accumulated to similar levels in cells infected with AD169, ΔUL97, and T2819 (Fig. 4d), with a complete block in virus yield (Fig. 4e). This finding was consistent with the drug's mechanism of action and with our previous results (82). However, following release from the drug-induced block, T2819 and ΔUL97 demonstrated ~2- and ~3-log reductions, respectively, in the yield of extracellular progeny virus compared to levels for the wild-type virus (Fig. 4e). These maintained differences in viral yield, despite the synchronization of DNA accumulation by the BDCRB-induced block, suggest that UL97 has both a kinase-mediated role (responsible for the 2-log reduction) and an additional nonkinase function (responsible for the additional 1-log reduction of ΔUL97 compared to the level for T2819) in the late phase of virus replication.

Distinct involvement of kinase-mediated and nonkinase functions of UL97 in cytoplasmic tegumentation and release. A detailed comparison of nuclear and cytoplasmic assembly intermediates in T2819, ΔUL97, and AD169, as well as NGIC-I-treated wild-type-infected cells, by transmission EM revealed no differences in nuclear encapsidation and no differences in nucleocytoplasmic egress between the deletion and the catalytically inactive virus. The nuclear accumulation of capsids, with an increased proportion of empty capsids, was noted in T2819-infected cells (Fig. 5A, image a, and Table 1). Similar results were obtained from cells infected with ΔUL97 (Table 1) (82). These findings, together with the paucity of DNA-containing C capsids in the cytoplasm of both T2819- and ΔUL97-infected cells, as well as in NGIC-I-treated AD169-infected cells, reflect the fact that the functions of UL97 in nuclear encapsidation and egress are kinase dependent. These results are in accordance with recent studies showing that lamin phosphorylation by UL97 mediates the dissolution of the nuclear lamina to promote nuclear egress (27, 49). Additionally, both T2819-infected cells and NGIC-I-treated AD169-infected cells demonstrated the formation of ΔUL97-like nuclear and cytoplasmic tegument aggregates and cytoplasmic membrane stacks (Fig. 5A, image b, and B, images a and b), indicating the specific relation of these features to the abrogation of UL97 kinase activity. Importantly, consistent differences in the proportions of strictly cytoplasmic assembly intermediates were found between T2819- and ΔUL97-infected cells based on the analysis of multiple representative fields from different sections. These included the increased proportion of DBs and tegumented capsids in T2819-infected cells and in NGIC-I-treated AD169-infected cells compared to the level for ΔUL97-infected cells (Fig. 5A, image c, and B, image a) (Table 1) and the presence of clusters of viral particles (Fig. 5A, image d, and Table 1), with the release of viral particles at the cell surface (not shown), which is completely absent from ΔUL97-infected cells (Fig. 1a and c and Table 1). Taken together, these results support the UL97 kinase-mediated roles in nuclear egress and cytoplasmic secondary envelopment and further reveal the additional contribution of a nonkinase function of UL97 to the formation, clustering, and release of tegumented viral forms.

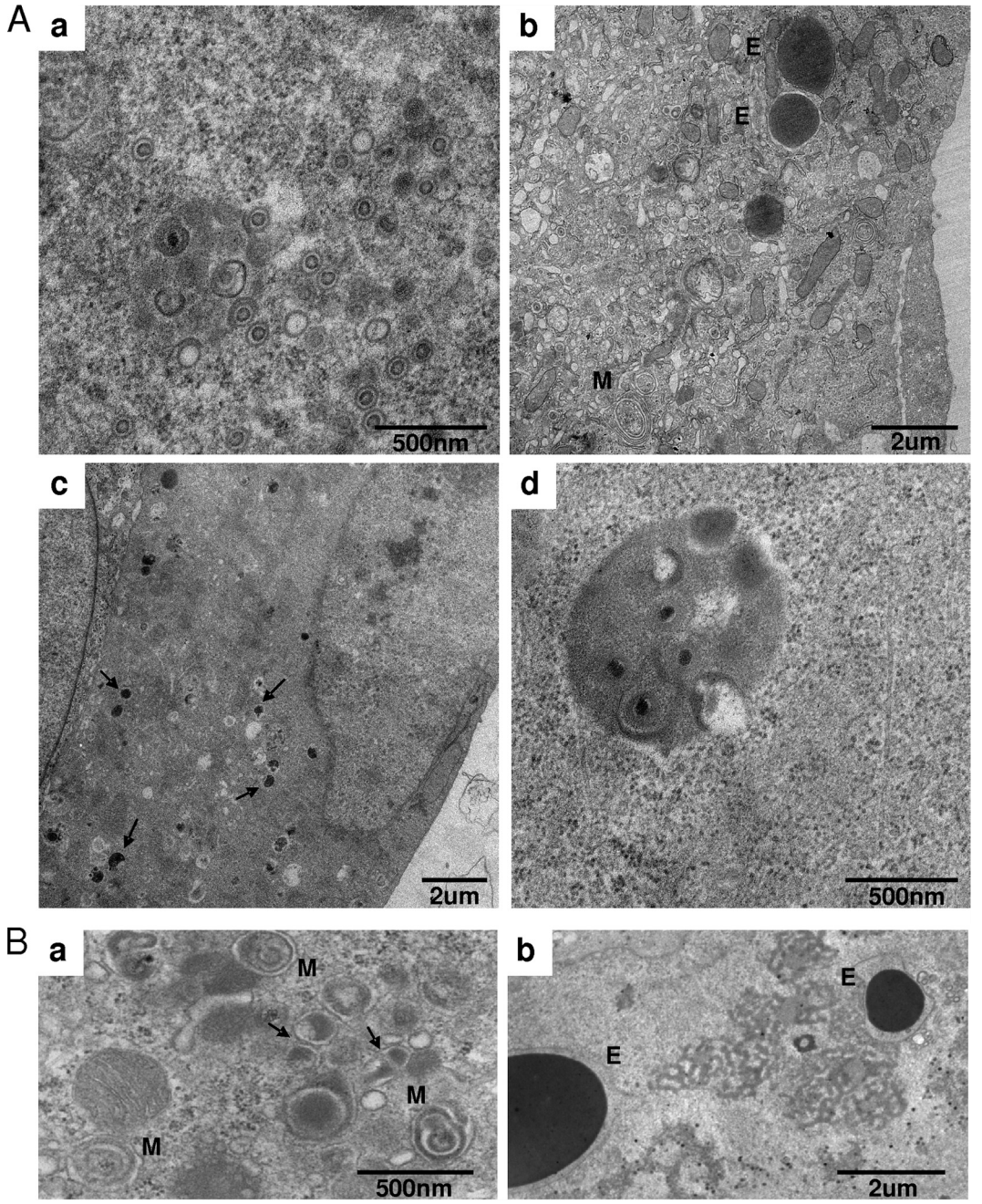

FIG. 5. Transmission electron microscopy of UL97 kinase-abrogated HCMV-infected HFF at 96 hpi. (A) T2819-infected HFF showing nucleus (a) and cytoplasm (b and d). Arrows in panel c point to dense bodies. (B) AD169-infected cells treated with NGIC-I. Arrows in panel a point to dense bodies. E, electron-dense structures. M, ovoid membrane stacks. Cells in the presented micrographs were fixed by standard fixation.

DISCUSSION

HCMV maturation and assembly follows a complex two-stage envelopment-and-egress process, which starts by encapsidation and primary envelopment in the nucleus and proceeds in the cytoplasm, where viral particles acquire their final tegument and envelope layers (secondary envelopment) at the cytoplasmic AC by budding through rearranged layers of cytoplasmic organelles. Mature virions and DBs are transported for release at the cell surface (22, 51, 56, 57). Our current understanding of the mechanisms driving the formation of the AC is limited, yet recent studies have started to uncover critical viral and cellular mediators of viral cytoplasmic assembly (1, 15, 31, 32, 42, 43, 47, 57, 72, 74, 75). The better interpretation of the role of specific alpha- and betaherpesvirus proteins in cytoplasmic assembly steps has been achieved by the use of deletion mutants, demonstrating the accumulation of aberrant cytoplasmic maturational intermediates and/or the absence of the pre-

dicted cytoplasmic maturational forms (1, 5, 11, 12, 14, 15, 31, 32, 33, 38, 39, 42, 43, 47, 57, 70, 72, 74, 75).

To date, the HCMV UL97 has been implicated primarily in nuclear maturation events (27, 40, 49, 55, 62, 63, 82). Here, we have conducted a comprehensive ultrastructural study of viral morphogenesis and thereby gained insight into a novel role of UL97 in cytoplasmic secondary envelopment. The involvement of UL97 in cytoplasmic assembly and tegumentation steps is suggested by a unique combination of ultrastructural features formed exclusively in cells infected with ΔUL97 or following the abrogation of UL97 kinase activity (by kinase-null K355M mutation or pharmacological inhibition): (i) aberrant cytoplasmic tegument aggregates, heavily stained for the major tegument proteins pp65 and pp28; (ii) distorted intracytoplasmic ovoid membrane structures, with abundant staining for the membrane-associated tegument protein pp28 (Fig. 1, 2, and 5); and (iii) a paucity of the expected cytoplasmic maturational forms, including tegumented capsids, dense bodies, and viral particle clusters. The formation of pp65-rich tegument aggregates extends our previous confocal microscopic analysis (2) and recent reports that demonstrated that the UL97 kinase impacts the cellular distribution of viral structural proteins and further identified a direct interaction between UL97 and pp65 (34, 63). While the abnormal aggregation of pp65 in the absence of UL97 kinase activity could result from the missing direct interaction between these two proteins, it is important to note that similar large intracytoplasmic aggregations of electron-dense tegument proteins also have been reported for cells infected by pseudorabies virus (PrV) gE, gI, and gM or UL11 mutants, in which secondary envelopment was almost completely blocked (11, 12, 38, 39). By analogy, this common feature could indicate a more general block in secondary envelopment in the absence of UL97. Moreover, the striking accumulation of aberrant membranes in the absence of UL97 kinase activity replaced the expected compartmentalized region of virus particles budding into orderly cytoplasmic membranes, which is observed in wild-type virus-infected cells. This altered morphology of pp28-bearing membranes is consistent with the modified distribution of pp28 and WGA ligands, as shown by our immunofluorescence studies (2), and could represent aborted cytoplasmic assembly complexes. To the best of our knowledge, this unique feature has not been described for any other HCMV maturation mutant so far. However, similar tightly connected, distorted membranes have been reported to form in the absence of the PrV membrane-associated UL11 protein (38, 39), the homolog of the HCMV pp28, which is known to mediate cytoplasmic assembly (57, 72). Interestingly, comparable morphological changes of cytoplasmic vesicles also were reported following the depletion of cellular proteins involved in lipid transport (44, 61). These peculiar similarities, reflecting altered biophysical properties and apposition between cytoplasmic membranes, could point to a role for UL97 in mediating efficient virus-induced vesicle trafficking or lipid transport via phosphorylation events.

Importantly, in cells infected with ΔUL97, very few virus particles accumulated in the cytoplasm, with a paucity of both tegumented nucleocapsids and clustered DBs. Whereas the absence of cytoplasmic nucleocapsids could result from the block in their nucleocytoplasmic translocation upon UL97 depletion, the reduced numbers of DBs could not be attributed to the missing nuclear functions of UL97; DBs are formed exclusively in the cytoplasm and presumably derive their envelope at the AC along with mature virions (57). The combined morphogenetic findings, i.e., the presence of aberrant tegument and cytoplasmic membrane aggregates, along with the impaired formation of maturational progeny, argue for the involvement of UL97 in common pathways of cytoplasmic assembly mediating the genesis of both tegumented capsids and DBs.

To further distinguish the cytoplasmic impact from the well-established role of UL97 in nuclear capsid maturation and egress, we examined the morphology of infected cells following the induction of an artificial block of encapsidation and nucleocytoplasmic egress by BDCRB treatment. Clearly, under these restrictions, none of the ΔUL97-like cytoplasmic characteristics could be noted, and DB formation and release appeared unimpaired or even excessive (Fig. 3). Moreover, cytoplasmic tegument aggregates and modified membrane structures were reinduced only upon a combined block with BDCRB and UL97 kinase inhibitor, specifically linking the cytoplasmic features to abrogated UL97 kinase activity and proving it unlikely that the cytoplasmic effects of UL97 deletion are due solely to impaired capsid maturation and nuclear egress. This finding could explain the synergistic antiviral activity reported for the combination of BDCRB with UL97 inhibitor (24) and further reinforce with precision that UL97 plays an additional role in downstream cytoplasmic maturation events.

To date, several HCMV tegument and envelope proteins, including pp150, pp28, gO, and gM/gN, have been shown to mediate viral cytoplasmic assembly and secondary envelopment (1, 5, 14, 32, 33, 42, 47, 57, 70, 72, 75). Maturation block mutants of these proteins demonstrated the impaired accumulation of capsids in the cytoplasm or the cytoplasmic accumulation of nonenveloped particles with reduced release of infectious progeny (32, 42, 47, 57, 72, 75). The diverging phenotypes of these mutants and the unique maturation block induced by UL97 abrogation highlight the complexity and the multicomponent nature of cytoplasmic secondary envelopment. Intriguingly, the absence of UL97 kinase activity is known to result in failure to remodel the nuclear lamina and rearrange the nucleus during infection (2, 27, 49, 54, 55). It is conceivable that the improper rearrangement of the nuclear lamins in the absence of UL97 affects the structure of adjacent AC components. Indeed, the presence of an integrated nucleocytoplasmic functional assembly and egress continuum recently has been suggested by the findings that the depletion of BiP and loss of AC integrity result in the loss of virus-induced nuclear lamina rearrangement, and that dynein is involved in both AC formation and the remodeling of the nuclear morphology in infected cells (15, 31). Hence, UL97, acting together with cell cycle kinases (28), may be a player in the coordinated signals interlinking nuclear remodeling and AC function integrity.

Thus far, the complex roles of UL97 in viral replication have been entirely attributed to its kinase activity, and multiple cellular and viral targets of UL97 have been identified (3, 4, 27, 30, 34, 36, 41, 48, 49, 65, 76). Accordingly, the deletion of UL97 and the specific abrogation of its kinase activity resulted in similar growth phenotypes under high-MOI conditions (2, 26, 30, 62). Surprisingly, however, we have found that under low-MOI conditions, viral yield inhibition by ΔUL97 was consis-

tently more extensive (by one order of magnitude) than that observed following the specific abrogation of UL97 kinase activity by either kinase-null point mutation or pharmacological inhibition. Further concurrent studies of viral growth and DNA accumulation during block and release with BDCRB confirmed the additional contribution of a nonkinase function of UL97 and confined it to late steps of virus maturation and release (Fig. 4). Interestingly, the only ultrastructural correlate and the likely basis for the difference in growth efficacy was a higher number of cytoplasmic DBs, tegumented capsids, and clustered viral particles observed upon the specific abrogation of the kinase activity compared to that of infection by ΔUL97 (Fig. 5 and Table 1). These findings identify a distinct nonkinase function of UL97, which under low-MOI conditions promotes the efficient assembly, clustering, and release of tegumented viral particles, possibly via protein-protein interactions that drive the intricate network of tegument incorporation. This function might be compensated for by viral or cellular factors present at higher MOIs. Such potential protein-protein interactions may involve pp65 and pUL69, recently shown to form a complex with UL97 (6, 34, 76), with the former further shown to affect the incorporation of both UL97 and pUL69 into virus particles (18).

Taken together, our findings reveal a novel role for UL97 in HCMV cytoplasmic secondary envelopment steps, with the further distinction of kinase-mediated function in the formation of the virus-induced AC, and a nonkinase function enhancing the efficacy of viral tegumentation and release. Further studies of UL97 interaction partners and phosphorylation targets, as well as the characterization of the nature and mechanism of the aggregated membranes, will provide insight into modes by which HCMV regulates nuclear and cytoplasmic assembly and egress steps.

ACKNOWLEDGMENTS

This work was supported by grants from the Israel Science Foundation (D.G.W.) and NIH grant AI39938 (S.C.).

The electron microscopy studies were conducted at the Irving and Cherna Moskowitz Center for Nano and Bio-Nano Imaging at the Weizmann Institute of Science.

REFERENCES

1. **AuCoin, D. P., G. B. Smith, C. D. Meiering, and E. S. Mocarski.** 2006. Betaherpesvirus-conserved cytomegalovirus tegument protein ppUL32 (pp150) controls cytoplasmic events during virion maturation. J. Virol. **80:** 8199–8210.
2. **Azzeh, M., A. Honigman, A. Taraboulos, A. Rouvinski, and D. G. Wolf.** 2006. Structural changes in human cytomegalovirus cytoplasmic assembly sites in the absence of UL97 kinase activity. Virology **354:**69–79.
3. **Baek, M. C., P. M. Krosky, Z. He, and D. M. Coen.** 2002. Specific phosphorylation of exogenous protein and peptide substrates by the human cytomegalovirus UL97 protein kinase. Importance of the P+5 position. J. Biol. Chem. **277:**29593–29599.
4. **Baek, M. C., P. M. Krosky, A. Pearson, and D. M. Coen.** 2004. Phosphorylation of the RNA polymerase II carboxyl-terminal domain in human cytomegalovirus-infected cells and in vitro by the viral UL97 protein kinase. Virology **324:**184–193.
5. **Baxter, M. K., and W. Gibson.** 2001. Cytomegalovirus basic phosphoprotein (pUL32) binds to capsids in vitro through its amino one-third. J. Virol. **75:**6865–6873.
6. **Becke, S., et al.** 2010. Modification of the major tegument protein pp65 of human cytomegalovirus inhibits viral growth and leads to the enhancement of a protein complex with pUL69 and pUL97 in infected cells. J. Gen. Virol.
7. **Biron, K. K.** 2006. Antiviral drugs for cytomegalovirus diseases. Antiviral Res. **71:**154–163.
8. **Biron, K. K., et al.** 2002. Potent and selective inhibition of human cytomegalovirus replication by 1263W94, a benzimidazole L-riboside with a unique mode of action. Antimicrob. Agents Chemother. **46:**2365–2372.
9. **Boeckh, M., et al.** 2004. Optimization of quantitative detection of cytomegalovirus DNA in plasma by real-time PCR. J. Clin. Microbiol. **42:**1142–1148.
10. **Borst, E. M., G. Hahn, U. H. Koszinowski, and M. Messerle.** 1999. Cloning of the human cytomegalovirus (HCMV) genome as an infectious bacterial artificial chromosome in Escherichia coli: a new approach for construction of HCMV mutants. J. Virol. **73:**8320–8329.
11. **Brack, A. R., J. M. Dijkstra, H. Granzow, B. G. Klupp, and T. C. Mettenleiter.** 1999. Inhibition of virion maturation by simultaneous deletion of glycoproteins E, I, and M of pseudorabies virus. J. Virol. **73:**5364–5372.
12. **Brack, A. R., et al.** 2000. Role of the cytoplasmic tail of pseudorabies virus glycoprotein E in virion formation. J. Virol. **74:**4004–4016.
13. **Britt, W.** 2007. CMV maturation and egress, p. 311–323. *In* A. M. Arvin, E. S. Mocarski, P. Moore, R. Whitley, K. Yamanishi, G. Campadelli-Fiume, and B. Roizman (ed.), Human herpesviruses: biology, therapy and immunoprophylaxis. Cambridge University Press, Cambridge, United Kingdom.
14. **Britt, W. J., M. Jarvis, J. Y. Seo, D. Drummond, and J. Nelson.** 2004. Rapid genetic engineering of human cytomegalovirus by using a lambda phage linear recombination system: demonstration that pp28 (UL99) is essential for production of infectious virus. J. Virol. **78:**539–543.
15. **Buchkovich, N. J., T. G. Maguire, and J. C. Alwine.** 2010. Role of the endoplasmic reticulum chaperone BiP, SUN domain proteins, and dynein in altering nuclear morphology during human cytomegalovirus infection. J. Virol. **84:**7005–7017.
16. **Cano-Monreal, G. L., K. M. Wylie, F. Cao, J. E. Tavis, and L. A. Morrison.** 2009. Herpes simplex virus 2 UL13 protein kinase disrupts nuclear lamins. Virology **392:**137–147.
17. **Chen, M. R., S. J. Chang, H. Huang, and J. Y. Chen.** 2000. A protein kinase activity associated with Epstein-Barr virus BGLF4 phosphorylates the viral early antigen EA-D in vitro. J. Virol. **74:**3093–3104.
18. **Chevillotte, M., et al.** 2009. Major tegument protein pp65 of human cytomegalovirus is required for the incorporation of pUL69 and pUL97 into the virus particle and for viral growth in macrophages. J. Virol. **83:**2480–2490.
19. **Chou, S.** 2009. Diverse cytomegalovirus UL27 mutations adapt to loss of viral UL97 kinase activity under maribavir. Antimicrob. Agents Chemother. **53:**81–85.
20. **Chou, S., L. C. Van Wechel, H. M. Lichy, and G. I. Marousek.** 2005. Phenotyping of cytomegalovirus drug resistance mutations by using recombinant viruses incorporating a reporter gene. Antimicrob. Agents Chemother. **49:** 2710–2715.
21. **Coller, K. E., and G. A. Smith.** 2008. Two viral kinases are required for sustained long distance axon transport of a neuroinvasive herpesvirus. Traffic **9:**1458–1470.
22. **Das, S., A. Vasanji, and P. E. Pellett.** 2007. Three-dimensional structure of the human cytomegalovirus cytoplasmic virion assembly complex includes a reoriented secretory apparatus. J. Virol. **81:**11861–11869.
23. **Erazo, A., and P. R. Kinchington.** 2010.Varicella-zoster virus open reading frame 66 protein kinase and its relationship to alphaherpesvirus US3 kinases. Curr. Top. Microbiol. Immunol. **342:**79–98.
24. **Evers, D. L., et al.** 2002. Interactions among antiviral drugs acting late in the replication cycle of human cytomegalovirus. Antiviral Res. **56:**61–72.
25. **Fraile-Ramos, A., et al.** 2002. Localization of HCMV UL33 and US27 in endocytic compartments and viral membranes. Traffic **3:**218–232.
26. **Gill, R. B., S. L. Frederick, C. B. Hartline, S. Chou, and M. N. Prichard.** 2009. Conserved retinoblastoma protein-binding motif in human cytomegalovirus UL97 kinase minimally impacts viral replication but affects susceptibility to maribavir. Virol. J. **6:**9.
27. **Hamirally, S., et al.** 2009. Viral mimicry of Cdc2/cyclin-dependent kinase 1 mediates disruption of nuclear lamina during human cytomegalovirus nuclear egress. PLoS Pathog. **5:**e1000275.
28. **Hertel, L., S. Chou, and E. S. Mocarski.** 2007. Viral and cell cycle-regulated kinases in cytomegalovirus-induced pseudomitosis and replication. PLoS Pathog. **3:**e6.
29. **Homman-Loudiyi, M., K. Hultenby, W. Britt, and C. Soderberg-Naucler.** 2003. Envelopment of human cytomegalovirus occurs by budding into Golgi-derived vacuole compartments positive for gB, Rab 3, trans-golgi network 46, and mannosidase II. J. Virol. **77:**3191–3203.
30. **Hume, A. J., et al.** 2008. Phosphorylation of retinoblastoma protein by viral protein with cyclin-dependent kinase function. Science **320:**797–799.
31. **Indran, S. V., M. E. Ballestas, and W. J. Britt.** 2010. Bicaudal D1-dependent trafficking of human cytomegalovirus tegument protein pp150 in virus-infected cells. J. Virol. **84:**3162–3177.
32. **Jiang, X. J., et al.** 2008. UL74 of human cytomegalovirus contributes to virus release by promoting secondary envelopment of virions. J. Virol. **82:**2802–2812.
33. **Jones, T. R., and S. W. Lee.** 2004. An acidic cluster of human cytomegalovirus UL99 tegument protein is required for trafficking and function. J. Virol. **78:**1488–1502.
34. **Kamil, J. P., and D. M. Coen.** 2007. Human cytomegalovirus protein kinase UL97 forms a complex with the tegument phosphoprotein pp65. J. Virol. **81:**10659–10668.
35. **Kato, A., et al.** 2006. Herpes simplex virus 1-encoded protein kinase UL13

phosphorylates viral Us3 protein kinase and regulates nuclear localization of viral envelopment factors UL34 and UL31. J. Virol. **80:**1476–1486.
36. **Kawaguchi, Y., T. Matsumura, B. Roizman, and K. Hirai.** 1999. Cellular elongation factor 1delta is modified in cells infected with representative alpha-, beta-, or gammaherpesviruses. J. Virol. **73:**4456–4460.
37. **Kenyon, T. K., and C. Grose.** 2010. VZV ORF47 serine protein kinase and its viral substrates. Curr. Top. Microbiol. Immunol. **342:**99–111.
38. **Kopp, M., H. Granzow, W. Fuchs, B. Klupp, and T. C. Mettenleiter.** 2004. Simultaneous deletion of pseudorabies virus tegument protein UL11 and glycoprotein M severely impairs secondary envelopment. J. Virol. **78:**3024–3034.
39. **Kopp, M., et al.** 2003. The pseudorabies virus UL11 protein is a virion component involved in secondary envelopment in the cytoplasm. J. Virol. **77:**5339–5351.
40. **Krosky, P. M., M. C. Baek, and D. M. Coen.** 2003. The human cytomegalovirus UL97 protein kinase, an antiviral drug target, is required at the stage of nuclear egress. J. Virol. **77:**905–914.
41. **Krosky, P. M., et al.** 2003. The human cytomegalovirus UL44 protein is a substrate for the UL97 protein kinase. J. Virol. **77:**7720–7727.
42. **Krzyzaniak, M., M. Mach, and W. J. Britt.** 2007. The cytoplasmic tail of glycoprotein M (gpUL100) expresses trafficking signals required for human cytomegalovirus assembly and replication. J. Virol. **81:**10316–10328.
43. **Krzyzaniak, M. A., M. Mach, and W. J. Britt.** 2009. HCMV-encoded glycoprotein M (UL100) interacts with Rab11 effector protein FIP4. Traffic **10:** 1439–1457.
44. **Lajoie, P., G. Guay, J. W. Dennis, and I. R. Nabi.** 2005. The lipid composition of autophagic vacuoles regulates expression of multilamellar bodies. J. Cell Sci. **118:**1991–2003.
45. **Lee, C. P., et al.** 2008. Epstein-Barr virus BGLF4 kinase induces disassembly of the nuclear lamina to facilitate virion production. J. Virol. **82:**11913–11926.
46. **Littler, E., A. D. Stuart, and M. S. Chee.** 1992. Human cytomegalovirus UL97 open reading frame encodes a protein that phosphorylates the antiviral nucleoside analogue ganciclovir. Nature **358:**160–162.
47. **Mach, M., et al.** 2007. The carboxy-terminal domain of glycoprotein N of human cytomegalovirus is required for virion morphogenesis. J. Virol. **81:** 5212–5224.
48. **Marschall, M., et al.** 2003. The protein kinase pUL97 of human cytomegalovirus interacts with and phosphorylates the DNA polymerase processivity factor pUL44. Virology **311:**60–71.
49. **Marschall, M., et al.** 2005. Cellular p32 recruits cytomegalovirus kinase pUL97 to redistribute the nuclear lamina. J. Biol. Chem. **280:**33357–33367.
50. **Marschall, M., et al.** 2001. Inhibitors of human cytomegalovirus replication drastically reduce the activity of the viral protein kinase pUL97. J. Gen. Virol. **82:**1439–1450.
51. **Mettenleiter, T. C.** 2002. Herpesvirus assembly and egress. J. Virol. **76:**1537–1547.
52. **Michel, D., and T. Mertens.** 2004. The UL97 protein kinase of human cytomegalovirus and homologues in other herpesviruses: impact on virus and host. Biochim. Biophys. Acta **1697:**169–180.
53. **Michel, D., et al.** 1996. The UL97 gene product of human cytomegalovirus is an early-late protein with a nuclear localization but is not a nucleoside kinase. J. Virol. **70:**6340–6346.
54. **Milbradt, J., S. Auerochs, and M. Marschall.** 2007. Cytomegaloviral proteins pUL50 and pUL53 are associated with the nuclear lamina and interact with cellular protein kinase C. J. Gen. Virol. **88:**2642–2650.
55. **Milbradt, J., S. Auerochs, H. Sticht, and M. Marschall.** 2009. Cytomegaloviral proteins that associate with the nuclear lamina: components of a postulated nuclear egress complex. J. Gen. Virol. **90:**579–590.
56. **Mocarski, E. S.** 2007. Betherpesvirus genes and their functions, p. 202–228. *In* A. M. Arvin, E. S. Mocarski, P. Moore, R. Whitley, K. Yamanishi, G. Campadelli-Fiume, and B. Roizman (ed.), Human herpesviruses: biology, therapy and immunoprophylaxis. Cambridge University Press, Cambridge, United Kingdom.
57. **Mocarski, E. S., T. Shenk, and R. F. Pass.** 2007. Cytomegaloviruses, p. 2702–2773. *In* D. M. Knipe and P. M. Howley (ed.), Fields virology, 5th ed., vol. II. Lippincott Williams & Wilkins, Philadelphia, PA.
58. **Moffat, J. F., et al.** 1998. The ORF47 and ORF66 putative protein kinases of varicella-zoster virus determine tropism for human T cells and skin in the SCID-hu mouse. Proc. Natl. Acad. Sci. U. S. A. **95:**11969–11974.
59. **Muranyi, W., J. Haas, M. Wagner, G. Krohne, and U. H. Koszinowski.** 2002. Cytomegalovirus recruitment of cellular kinases to dissolve the nuclear lamina. Science **297:**854–857.
60. **Ng, T. I., L. Keenan, P. R. Kinchington, and C. Grose.** 1994. Phosphorylation of varicella-zoster virus open reading frame (ORF) 62 regulatory product by viral ORF 47-associated protein kinase. J. Virol. **68:**1350–1359.
61. **Peretti, D., N. Dahan, E. Shimoni, K. Hirschberg, and S. Lev.** 2008. Coordinated lipid transfer between the endoplasmic reticulum and the Golgi complex requires the VAP proteins and is essential for Golgi-mediated transport. Mol. Biol. Cell **19:**3871–3884.
62. **Prichard, M. N.** 2009. Function of human cytomegalovirus UL97 kinase in viral infection and its inhibition by maribavir. Rev. Med. Virol. **19:**215–229.
63. **Prichard, M. N., W. J. Britt, S. L. Daily, C. B. Hartline, and E. R. Kern.** 2005. Human cytomegalovirus UL97 Kinase is required for the normal intranuclear distribution of pp65 and virion morphogenesis. J. Virol. **79:**15494–15502.
64. **Prichard, M. N., et al.** 1999. A recombinant human cytomegalovirus with a large deletion in UL97 has a severe replication deficiency. J. Virol. **73:**5663–5670.
65. **Prichard, M. N., et al.** 2008. Human cytomegalovirus UL97 kinase activity is required for the hyperphosphorylation of retinoblastoma protein and inhibits the formation of nuclear aggresomes. J. Virol. **82:**5054–5067.
66. **Purves, F. C., W. O. Ogle, and B. Roizman.** 1993. Processing of the herpes simplex virus regulatory protein alpha 22 mediated by the UL13 protein kinase determines the accumulation of a subset of alpha and gamma mRNAs and proteins in infected cells. Proc. Natl. Acad. Sci. U. S. A. **90:**6701–6705.
67. **Roizman, B., D. M. Knipe, and R. J. Whitley.** 2007. Herpes simplex viruses, p. 2503–2602. *In* D. M. Knipe and P. M. Howley (ed.), Fields virology, 5th ed., vol. II. Lippincott Williams & Wilkins, Philadelphia, PA.
68. **Romaker, D., et al.** 2006. Analysis of the structure-activity relationship of four herpesviral UL97 subfamily protein kinases reveals partial but not full functional conservation. J. Med. Chem. **49:**7044–7053.
69. **Sanchez, V., K. D. Greis, E. Sztul, and W. J. Britt.** 2000. Accumulation of virion tegument and envelope proteins in a stable cytoplasmic compartment during human cytomegalovirus replication: characterization of a potential site of virus assembly. J. Virol. **74:**975–986.
70. **Seo, J. Y., and W. J. Britt.** 2007. Cytoplasmic envelopment of human cytomegalovirus requires the postlocalization function of tegument protein pp28 within the assembly compartment. J. Virol. **81:**6536–6547.
71. **Shapira, M. Y., et al.** 2008. Artesunate as a potent antiviral agent in a patient with late drug-resistant cytomegalovirus infection after hematopoietic stem cell transplantation. Clin. Infect. Dis. **46:**1455–1457.
72. **Silva, M. C., Q. C. Yu, L. Enquist, and T. Shenk.** 2003. Human cytomegalovirus UL99-encoded pp28 is required for the cytoplasmic envelopment of tegument-associated capsids. J. Virol. **77:**10594–10605.
73. **Sullivan, V., et al.** 1992. A protein kinase homologue controls phosphorylation of ganciclovir in human cytomegalovirus-infected cells. Nature **358:**162–164.
74. **Tandon, R., D. P. AuCoin, and E. S. Mocarski.** 2009. Human cytomegalovirus exploits ESCRT machinery in the process of virion maturation. J. Virol. **83:**10797–10807.
75. **Tandon, R., and E. S. Mocarski.** 2008. Control of cytoplasmic maturation events by cytomegalovirus tegument protein pp150. J. Virol. **82:**9433–9444.
76. **Thomas, M., et al.** 2009. Cytomegaloviral protein kinase pUL97 interacts with the nuclear mRNA export factor pUL69 to modulate its intranuclear localization and activity. J. Gen. Virol. **90:**567–578.
77. **Tooze, J., M. Hollinshead, B. Reis, K. Radsak, and H. Kern.** 1993. Progeny vaccinia and human cytomegalovirus particles utilize early endosomal cisternae for their envelopes. Eur. J. Cell Biol. **60:**163–178.
78. **Underwood, M. R., et al.** 1998. Inhibition of human cytomegalovirus DNA maturation by a benzimidazole ribonucleoside is mediated through the UL89 gene product. J. Virol. **72:**717–725.
79. **van Zeijl, M., J. Fairhurst, E. Z. Baum, L. Sun, and T. R. Jones.** 1997. The human cytomegalovirus UL97 protein is phosphorylated and a component of virions. Virology **231:**72–80.
80. **Varnum, S. M., et al.** 2004. Identification of proteins in human cytomegalovirus (HCMV) particles: the HCMV proteome. J. Virol. **78:**10960–10966.
81. **Warming, S., N. Costantino, D. L. Court, N. A. Jenkins, and N. G. Copeland.** 2005. Simple and highly efficient BAC recombineering using galK selection. Nucleic Acids Res. **33:**e36.
82. **Wolf, D. G., C. T. Courcelle, M. N. Prichard, and E. S. Mocarski.** 2001. Distinct and separate roles for herpesvirus-conserved UL97 kinase in cytomegalovirus DNA synthesis and encapsidation. Proc. Natl. Acad. Sci. U. S. A. **98:**1895–1900.
83. **Wolf, D. G., et al.** 2003. Emergence of late cytomegalovirus central nervous system disease in hematopoietic stem cell transplant recipients. Blood **101:** 463–465.
84. **Zacny, V. L., E. Gershburg, M. G. Davis, K. K. Biron, and J. S. Pagano.** 1999. Inhibition of Epstein-Barr virus replication by a benzimidazole L-riboside: novel antiviral mechanism of 5,6-dichloro-2-(isopropylamino)-1-beta-L-ribofuranosyl-1H-benzimidazole. J. Virol. **73:**7271–7277.